

AN OPEN SOURCE MECHANISTIC MODEL FOR CO<sub>2</sub> / H<sub>2</sub>S CORROSION OF CARBON STEEL

Srdjan Nešić<sup>(1)</sup>, Hui Li, Jing Huang and Dusan Sormaz

Institute for Corrosion and Multiphase Technology

Department of Chemical Engineering

Ohio University

Athens, OH 45701

**ABSTRACT**

A mechanistic model is developed to predict the corrosion rate caused by CO<sub>2</sub>, H<sub>2</sub>S, organic acids and/or O<sub>2</sub>. The aim of this model was to provide the corrosion community with a theoretically sound, simple and effective corrosion model for internal corrosion of mild steel lines. This model is available in the open literature and can be easily accessed on the internet. All the background information, including theories behind, data used for calibration, limitations, etc. is shared with users. In addition, the source code of the model, which has been written in object-oriented fashion, is open to the public to encourage utilization of any individual modules and development of add-on modules by third parties.

The main features of this model include: prediction of uniform corrosion rate by CO<sub>2</sub>, H<sub>2</sub>S, organic acids and/or O<sub>2</sub>, simulation of iron carbonate film and iron sulfide film growth, identification of major corrosive species by quantifying respective contributions from various species, capability of distinguishing CO<sub>2</sub>/ H<sub>2</sub>S dominant corrosion processes, display and manipulation of polarization curves for CO<sub>2</sub> dominant processes, or display of H<sub>2</sub>S concentration profile as a function of distance from steel surface for H<sub>2</sub>S dominant processes, capability of modifying the corrosion calculation process by adding user-defined reactions or excluding any undesired reactions.

**Keywords:** mechanistic model, corrosion prediction, CO<sub>2</sub> corrosion, H<sub>2</sub>S corrosion, HAc corrosion

---

<sup>(1)</sup> Corresponding author, E-mail address: nesic@ohio.edu (S. Nestic).

Copyright

©2009 by NACE International. Requests for permission to publish this manuscript in any form, in part or in whole must be in writing to NACE International, Copyright Division, 1440 South creek Drive, Houston, Texas 777084. The material presented and the views expressed in this paper are solely those of the author(s) and are not necessarily endorsed by the Association. Printed in the U.S.A.

# INTRODUCTION

Carbon steel is extensively used in oil and gas pipelines due to the merit of low cost. These pipelines are frequently exposed to the aqueous environments containing aggressive species, such as CO<sub>2</sub>, H<sub>2</sub>S and organic acids which pose significant threat to the normal operation of pipelines. Intense research efforts have been made with the aim of understanding corrosion mechanisms caused by various corrosive species and factors that either promote or inhibit corrosion. As a result, a large number of publications have become available which deal with corrosion from different aspects. Although some issues remain unclear, most of the steps that are associated with CO<sub>2</sub> and to a lesser degree H<sub>2</sub>S corrosion process are now understood. With available information, it is possible to establish a mechanistic model to predict corrosion rate and help further the understanding of corrosion process. In fact, a number of corrosion models for CO<sub>2</sub> corrosion in wells and pipelines have been developed in recent years<sup>1</sup>. However, these models, most of which are proprietary and unavailable to public, often give a large scatter in the prediction due to different theories, assumptions and modeling strategies. This is aggravated by lack of transparency of the code behind the models. When more corrosive species are involved in the corrosion process, larger discrepancies are to be expected from various models. The project presented in this paper aimed at providing the corrosion community with a free mechanistic model for internal corrosion prediction of carbon steel pipelines. Strongly rooted in theories, this model can offer trustworthy predictions for a wide range of conditions that are typical for oil and gas pipelines, as will be shown in the following sections. This model, named FREECORP<sup>(2)</sup>, was developed exclusively based on public information. All the information related to the model, including theories, assumptions, limitations and data used for calibration are shared with the users. To maximize the transparency of the model, the source code is also shared. With source code available, further development of the model can be easily achieved by adding new modules or by modifying existing modules. This provides a way to serve special needs that the users might have in their unique corrosion environments.

This model is available in the open literature and can be easily accessed on the internet (<http://www.corrosioncenter.ohiou.edu/freecorp>). Being offered to the corrosion community, this model will hopefully:

- Elevate the level of understanding and the prediction capability of mild steel corrosion as related to the oil and gas industry.
- Ensure that best available science and technology is available to the corrosion engineers, implemented by using a transparent approach which is open for further development and improvement.
- Increase the level of involvement of the broader corrosion community in developing better and more flexible tools fit for their intended purposes, an approach which will hopefully be mimicked in the future in other fields of corrosion.
- Fulfill one of the key missions of the Institute for Corrosion and Multiphase Technology and Ohio University as a public institution: to educate the wider professional community and extend its reach beyond the pool of the current research sponsors in order to enable more effective dissemination of the already published knowledge and technology.

---

<sup>(2)</sup> FREECORP is a product of the Institute for Corrosion and Multiphase Technology, Ohio University distributed under the GNU General Public License.

The model presented in this paper is capable of predicting uniform corrosion rate of carbon steel in the environment containing carbon dioxide, hydrogen sulfide, organic acid and/or oxygen. Respective contributions of various corrosive species are calculated which enables the identification of major corrosive species. Potentiodynamic sweep curve or H<sub>2</sub>S concentration profile is also shown depending on the dominating corrosion mechanism, which helps further elucidate the corrosion mechanism. The effect of iron carbonate growth is simulated using empirical relationships to enhance the accuracy of predictions.

In the following sections, main theories of corrosion caused by carbon dioxide, hydrogen sulfide, organic acid and/or oxygen are reviewed, followed by implementation of the model. The model is then compared with experimental results under various conditions. In the final section, the limitations associated with the current version of the model are stated and the directions for future development are suggested.

## THEORIES OF THE MODEL

The theories and equations used in this model are attributed to various publications. Nonetheless, the main theories that serve as the basis of the present model are taken from three key papers<sup>2,3,4</sup>. To help understand the process described in the model, a brief review of the theories involved is given here. Detailed information about the corrosion process can be found in the original papers.

### Carbon Dioxide/ Acetic Acid Corrosion

Carbon dioxide corrosion is a complicated process in which a number of chemical reactions, electrochemical reactions and transport processes occur simultaneously.<sup>2</sup>

Chemical reactions. Carbon dioxide is often present in the oil and gas pipelines. Various chemical reactions take place in the water phase due to the presence of carbon dioxide. These reactions have to be taken into consideration in order to get the accurate concentrations of corrosive species for further calculation.

CO<sub>2</sub> is soluble in water:



Hydration of aqueous CO<sub>2</sub> produces a weak acid, known as carbonic acid, H<sub>2</sub>CO<sub>3</sub>:



Carbonic acid can then partially dissociate in two steps to form bicarbonate and carbonate ions:



Homogenous dissociation reactions (3) and (4) proceed much faster than the other simultaneously occurring processes in the system. CO<sub>2</sub> dissolution reaction (1) and particularly CO<sub>2</sub> hydration reaction

(2) have been known to be much slower (rate controlling) and could lead to local non-equilibrium in the solution.

In some environments organic acids, particularly low molecular weight organic acids, are found primarily in water phase and can lead to corrosion of mild steel. Acetic acid, (*HAc*) which is the most prevalent type of organic acids found in brines, can be treated as the representative of other types of organic acids as similar corrosiveness was found for all types of low molecular weight organic acids.

*HAc* is a weak acid which is rather volatile – a property that makes it a major concern in top-of-line corrosion (TLC). It partially dissociates in the water phase to give away  $H^+$  and  $Ac^-$ , as indicated by reaction (5). However it is stronger than  $H_2CO_3$ , and therefore serves as the main source of  $H^+$  when similar concentration of the two acids are encountered.



In the temperature range of interest (20 – 100°C), *HAc* is mainly found in the aqueous phase and therefore corrosion caused by *HAc* is not strongly affected by presence of *HAc* vapors (other than in the case of TLC). This is different from  $CO_2$  corrosion where gaseous  $CO_2$  controls the amount of  $H_2CO_3$  in the aqueous phase and therefore determines the rate of  $CO_2$  corrosion.

Another important chemical reaction that needs special attention is the formation of iron carbonate in the circumstance where concentrations of ferrous ion and carbonate ion exceed the solubility limit of iron carbonate, as indicated by reaction (6):



This reaction is a heterogeneous reaction as nucleation of solid iron carbonate occurs preferably on the steel surface or inside the pores of the present film.

The precipitation of  $FeCO_{3(s)}$  often plays a significant role in the corrosion process because the  $FeCO_{3(s)}$  layer may increase the mass transfer resistance for the corrosive species as well as reduce the available steel surface exposed to the corrosive solution. In fact, in many cases, the  $CO_2$  corrosion rate is largely controlled by the presence of the  $FeCO_{3(s)}$  layer.

Electrochemical reactions. For  $CO_2$  corrosion, several electrochemical reactions have been identified as contributors to overall corrosion rate of mild steel.

Dissolution of iron is the dominant anodic reaction. This reaction proceeds via a multi-step mechanism which is mildly affected by pH and  $CO_2$  concentration. In the range of typical  $CO_2$  corrosion, e.g. pH >4, the dependency of pH tends to diminish. Therefore, for practical purposes, this reaction can be treated as pH independent for  $CO_2$  corrosion. At the corrosion potential (and up to 200 mV above), this reaction is under charge transfer control and therefore the electrochemical behavior can be described using Tafel's law.



Hydrogen ion,  $H^+$ , reduction is one of the main cathodic processes:



This reaction is limited by how fast the  $H^+$  can be transported from the bulk solution to the steel surface through the mass transfer layer (including liquid boundary layer and the  $FeCO_3(s)$  layer if it exists). Higher corrosion rates are often experimentally observed for  $CO_2$  system comparing to strong acid solution (such as HCl) at the same pH. However, for practical  $CO_2$  system where  $pH > 4$ , the limiting flux of this reaction would be small due to the relative low concentration of  $H^+$ . This suggests that  $CO_2$  also plays certain role in  $H^+$  reduction. This can be explained by the fact that the homogeneous dissociation of  $H_2CO_3$  provides an additional reservoir for  $H^+$  ions, which then adsorbs on the steel surface and gets reduced according to reaction (8). Apparently, any rapid consumption of  $H^+$  can be readily replenished by reactions (3) and (4). Thus for  $pH > 4$  the presence of  $CO_2$  leads to a much higher corrosion rate than would be found in a solution of a strong acid at the same pH.

In the vicinity of the steel surface, another electrochemical reaction can take place as well:  $H_2CO_3$  adsorbs at the steel surface and is directly reduced according to reaction (9). This is referred to as “direct reduction of carbonic acid”<sup>5</sup>. In fact, this reaction is just an alternative pathway for the same cathodic reaction - hydrogen evolution as addition of reaction (3) and (8) leads to reaction (9). The distinction is only in the pathway, i.e in the sequence of reactions.



The rate of this additional hydrogen evolution due to the presence of  $CO_2$  is mainly controlled by the slow  $CO_2$  hydration step (2) and is a strong function of  $H_2CO_3$  concentration which directly depends on partial pressure of  $CO_2$ .

Although oxygen is not a common corrosive specie in oil and gas pipeline systems, it can invade the system by inappropriate operation or incomplete de-oxygenation of water chemical solutions injected into the system. Oxygen can contribute to corrosion process by oxygen reduction reaction which is limited by transport of oxygen through the mass transfer layer, as shown below:



Acetic acid is known to be one of the species that attacks mild steel. Studies have shown that it is the undissociated (“free”) HAc and not the acetate ion  $Ac^-$  that is responsible for corrosion. The presence of organic acids is a major corrosion concern particularly at lower pH and high temperature as more HAc would be generated under these conditions according to reaction (5).

Being a weak i.e. partially dissociated acid, HAc provides an additional source of  $H^+$ , which then adsorbs at the steel surface and reduces according to the cathodic reaction (8). Following the reasoning with  $H_2CO_3$ , it is also possible that the HAc molecule itself is adsorbed at the steel surface and gets reduced, which is often referred to as the “direct HAc reduction” pathway:



Another possible pathway for hydrogen evolution is direct reduction of water:



Compared to the cathodic reactions described above, this pathway is very slow and often can be neglected in practical CO<sub>2</sub> corrosion environments. However, under peculiar conditions, such as very low partial pressure of CO<sub>2</sub> ( $P_{CO_2} \ll 0.1$  bar) and high pH (pH >6), this reaction may become significant and contribute to the overall corrosion process. Therefore, even if rarely relevant, this reaction has been included in the model for completeness.

Transport. Due to electrochemical reactions, certain species are produced or consumed on the steel surface. Concentration gradients are therefore established between bulk solution and steel surface, which leads to molecular diffusion. In addition, pipelines are often subject to turbulent flow. Turbulent eddies can usually penetrate into the boundary layer and greatly enhance the transport of species. Compared to some fast electrochemical reactions, such as hydrogen evolution (8), mass transfer of  $H^+$  proceeds much slower and therefore the rates of the overall reaction will be limited by transport, i.e. how fast the species can move through the mass transfer layer and any solid corrosion product layer. It is therefore essential to incorporate transport phenomenon into the model in order to give an accurate description of the overall corrosion process. The effect of mass transport can be readily captured by using the concept of mass transfer coefficients.

### Numerical calculation for CO<sub>2</sub>/HAc corrosion

CO<sub>2</sub> and HAc corrosion are both electrochemical process. The corrosion rate can therefore be calculated based on total current density of the anodic reaction (or the sum of cathodic reactions).

$$CR = \frac{i_a M_{w,Fe}}{\rho_{Fe} nF} \quad (13)$$

Where,

$CR$ : corrosion rate, unit conversion factors are needed for appropriate unit;

$i_a$ : anodic current density, A/m<sup>2</sup>;

$M_{w,Fe}$ : atomic mass of iron, kg/mol;

$\rho_{Fe}$ : density of iron, kg/m<sup>3</sup>;

$n$ : number of moles of electrons involved in iron oxidation, 2 mol<sub>e</sub>/mol;

$F$ : Faraday's constant.

The anodic current density of iron oxidation is obtained by,

$$i_{a,Fe} = i_{o,Fe} \times 10^{\frac{E_{corr} - E_{rev,Fe}}{b_{Fe}}} \quad (14)$$

Where,

$i_{a,Fe}$ : current density of iron oxidation, A/m<sup>2</sup>;

$i_{o,Fe}$ : exchange current density of iron oxidation, A/m<sup>2</sup>;

$E$ : corrosion potential, V;

$E_{rev,Fe}$ : reversible potential of iron oxidation, V;

$b_{Fe}$ : Tafel slope of iron oxidation, V.

The current density of individual cathodic reaction is given by,

$$\frac{1}{i_c} = \frac{1}{i_{ct}} + \frac{1}{i_{lim}} \quad (15)$$

Where,

- $i_c$  : current density of any cathodic reaction, A/m<sup>2</sup>;
- $i_{ct}$  : component of charge transfer current density, A/m<sup>2</sup>;
- $i_{lim}$  : component of limiting current density, A/m<sup>2</sup>;

The charge transfer current density of cathodic reactions can be calculated by,

$$i_{ct} = i_o \times 10^{\frac{E_{rev} - E_{corr}}{b}} \cdot \eta_{FeCO_3} \cdot \eta_{FeS} \quad (16)$$

Where,

- $i_o$  : exchange current density of cathodic reactions, A/m<sup>2</sup>;
- $E_{rev}$  : reversible potential of cathodic reactions, V;
- $b$  : Tafel slope of cathodic reactions, V;
- $\eta_{FeCO_3}, \eta_{FeS}$  : scale factors due to formation of FeCO<sub>3</sub> and FeS film, respectively.

Most of cathodic reactions are mass transfer limited. The limiting current density can be calculated as,

$$i_{lim}^d = \eta_{FeCO_3} \cdot \eta_{FeS} \cdot k_m F c_j \quad (17)$$

Where,

- $k_m$  : mass transfer coefficient of corrosive species, m/s;
- $c_j$  : bulk concentration of corrosive species, mol/m<sup>3</sup>;

However, carbonic acid reduction is limited by slow reaction rate of CO<sub>2</sub> hydration, as shown in reaction 2. The limiting current density of this reaction is calculated in a different fashion, as shown below,

$$i_{lim, H_2CO_3}^r = F c_{CO_2} \left( \eta_{FeCO_3} \cdot \eta_{FeS} \cdot D_{H_2CO_3} K_{hyd} k_{hyd}^f \right)^{0.5} f \quad (18)$$

Where,

- $c_{CO_2}$  : concentration of CO<sub>2</sub> in bulk solution, mol/m<sup>3</sup>;
- $D_{H_2CO_3}$  : diffusion coefficient of H<sub>2</sub>CO<sub>3</sub> in water, m<sup>2</sup>/s;
- $k_{m, H_2CO_3}$  : mass transfer coefficient of H<sub>2</sub>CO<sub>3</sub>, m/s;
- $K_{hyd}$  : equilibrium constant for CO<sub>2</sub> hydration reaction;
- $k_{hyd}^d$  : forward reaction rate constant for CO<sub>2</sub> hydration reaction;
- $f$  : flow factor affecting CO<sub>2</sub> hydration, which is given by,

$$f = \frac{1 + e^{-2\delta_m / \delta_r}}{1 - e^{-2\delta_m / \delta_r}} \quad (19)$$

Where  $\delta_m$  and  $\delta_r$  are defined as mass transfer and reaction layer thickness, respectively, and can be calculated as,

$$\delta_m = \frac{D_{H_2CO_3}}{k_{m,H_2CO_3}} \quad (20)$$

$$\delta_r = \sqrt{\frac{D_{H_2CO_3} K_{hyd}}{k_{hyd}^f}} \quad (21)$$

The unknown corrosion potential,  $E_{corr}$ , can be found based on charge balance on the steel surface.

$$\sum_1^{na} i_a = \sum_1^{nc} i_c \quad (22)$$

Where,

$i_a, i_c$ : anodic and cathodic current density, respectively, A/m<sup>2</sup>;  
 $n_a, n_c$ : total numbers of anodic and cathodic reactions, respectively.

Once the corrosion potential is found, the corrosion current density can be calculated by using equation (14) as iron oxidation is normally the only one anodic reaction involved in the corrosion process even though the number of cathodic reactions is variable depending on the corrosive environment.

### Hydrogen Sulfide Corrosion

In contrast with CO<sub>2</sub> corrosion, which is electrochemical in nature, H<sub>2</sub>S corrosion of mild steel is considered to proceed predominantly via a *solid state* reaction:



The term *solid state* reaction refers to the fact that both initial and final state of iron are solid.

A plausible mechanism for H<sub>2</sub>S corrosion of mild steel proposed by Sun et. al.<sup>4</sup> is adopted in this model. According to this theory, H<sub>2</sub>S initially absorbed onto the steel surface reacts very fast with iron to form a very thin ( $\ll 1 \mu m$ ), dense and protective non-stoichiometric iron sulfide film – mackinawite. Due to its compactness, this film acts as a solid state diffusion barrier for species involved in the corrosion process which leads to a significant and rapid reduction of the corrosion rate. However, the diffusion of the corrosive species through this mackinawite film does not completely stop and the continuing corrosion at the steel surface keeps on generating more mackinawite. As this process proceeds, the internal stress in the mackinawite film is built up due to epitaxial stresses and the Pilling-Bedford ratio which is defined in this case as the ratio of the molar volumes of the mackinawite to the iron. Apparently, mackinawite has a much larger volume when compared to iron. These stresses lead to microcracking and eventually delamination of the mackinawite film. A cyclic process of growth, cracking and delaminating of mackinawite eventually leads to formation of an outer mackinawite layer which is thicker, more porous and less protective. Over time, the mackinawite might transform into other forms of sulfide such as pyrrhotite. In addition pyrrhotite might precipitate from the solution; however this

effect is not included in the present version of the model. The same is true for formation of pyrite and elemental sulfur which are not considered in the present version of the model. The mechanism described here is probably not the only way in which H<sub>2</sub>S corrosion happens. The model is open to take into consideration other mechanisms as more knowledge about this topic is gained.

It is apparent that, according to the above scenario, H<sub>2</sub>S corrosion is largely limited by how fast corrosive species can move through the iron sulfide layers present on the steel surface. Therefore, in the present model, H<sub>2</sub>S corrosion is always considered to be under mass transfer control. In addition, it is assumed that the presence of the mackinawite layers affects any other corrosive species such as CO<sub>2</sub> and organic acid in a similar fashion.

### Numerical Calculation for H<sub>2</sub>S corrosion

Corrosion by H<sub>2</sub>S is assumed to be under pure mass transfer control due to the presence of mackinawite layers and the liquid boundary layer. The flux of H<sub>2</sub>S through the mass transfer boundary layer, the porous outer mackinawite layer and the inner mackinawite film can be calculated as:

$$Flux_{H_2S} = k_{m(H_2S)}(c_{H_2S} - c_{o(H_2S)}) \quad (24)$$

$$Flux_{H_2S} = \frac{D_{H_2S}\varepsilon\psi}{\delta_{os}}(c_{o(H_2S)} - c_{i(H_2S)}) \quad (25)$$

$$Flux_{H_2S} = A_{H_2S} \ln\left(\frac{c_{i(H_2S)}}{c_{s(H_2S)}}\right) \quad (26)$$

respectively.

At steady state, the fluxes through different layers are equal to each other and equivalent to the corrosion rate. Thus, the corrosion rate caused by H<sub>2</sub>S can be obtained by equating equations (24) through (26). The final expression for the corrosion rate of H<sub>2</sub>S is given by equation (27):

$$CR_{H_2S} = A_{H_2S} \ln \frac{c_{b,H_2S} - Flux_{H_2S} \left( \frac{\delta_{os}}{D_{H_2S}\varepsilon\psi} + \frac{1}{k_{m,H_2S}} \right)}{c_{s,H_2S}} \quad (27)$$

Where,

$CR_{H_2S}$  : corrosion rate caused by H<sub>2</sub>S expressed in mol/(m<sup>2</sup>s);

$k_{m,H_2S}$  : mass transfer coefficient of H<sub>2</sub>S in liquid boundary layer, m/s;

$D_{H_2S}$  : diffusion coefficient of H<sub>2</sub>S in water;

$\varepsilon, \psi$  : porosity and tortuosity of outer mackinawite scale;

$\delta_{os}$  : thickness of the outer scale, m;

$c_{b,H_2S}, c_{s,H_2S}$  : concentration of H<sub>2</sub>S in bulk solution and at steel surface, respectively, mol/m<sup>3</sup>;

$A_{H_2S}$  : constant for solid state diffusion.

In the presence of  $H_2S$  the corrosion by other species such as  $H^+$ ,  $H_2CO_3$  and  $HAc$  etc., is also limited by mass transfer due to the presence of mackinawite and liquid boundary layers, therefore, the corrosion rates caused by these species are calculated in a similar fashion as that for  $H_2S$  (equation (27) ) by using different physical properties as appropriate.

## MODEL IMPLEMENTATION

### Model Construction

The model is available in the form of Excel add-in, which can be accessed from any Excel file without duplicating the code. This feature enables users to readily manipulate the input and output data by using plenty of functions provided by Microsoft Excel<sup>®(3)</sup>. The object-oriented programming (OOP) concepts are adopted in developing the code making the program structured in a highly organized fashion. For  $CO_2$  corrosion, the major calculation processes are treated as individual objects, which are separated from the graphic user interface (GUI) of the program and can be integrated into any external programs to serve special needs. In the current version of the code, the  $H_2S$  corrosion model has not been modularized to the same extent, a feature which will be improved in the near future. The architecture of the model is schematically shown in FIGURE 1.

### Main Features of the Model

One of the main features of the model is that the contribution of corrosive species to overall corrosion rate can be quantified. The contributions, which are expressed in percent, are calculated based on individual cathodic reaction rate for electrochemical process (such as  $CO_2$  corrosion) or flux of corrosive species for  $H_2S$  corrosion. This feature gives users a tool to identify the major corrosive species and facilitate the analysis of corrosion mechanism.

The corrosion mechanism can be further investigated by taking advantage of the curves given by the model. For electrochemical processes, polarization curves are provided for individual electrochemical reactions, total anodic and cathodic reactions. In addition, the potentiodynamic sweep can also be displayed. Each of these curves can be chosen to be visible or invisible to gain a better observation. For  $H_2S$  corrosion, the concentration profile of  $H_2S$  as a function of distance from steel surface is given since mass transfer is a major concern in this case. By comparing the concentration gradient across three different layers, e.g. inner mackinawite film, outer porous layer and liquid boundary layer, users can understand which layer offers the highest mass transfer resistance, and therefore plays the most significant role in the corrosion process.

Another unique feature of the model is that the advanced users are allowed to modify the calculation process by adding/ removing reactions, including adding new user-defined reactions into the electrochemical model. This feature enables the users to explore how one or more reactions, including user-defined reactions, affect the corrosion process. By accommodating user-defined reactions, a great deal of flexibility is provided by the model to deal with various corrosive environments besides the  $CO_2/H_2S$  system. A maximum of 10 anodic reactions and 10 cathodic reactions are allowed to participate in any corrosion calculation. The same flexibility is not built into the  $H_2S$  module in the present version of the code.

---

<sup>(3)</sup> Microsoft Excel is a trademarked product of Microsoft.

## MODEL VERIFICATION

This model has been extensively compared with experimental data from many sources. The main data source for comparison was taken from the ICMT database of over 700 unique cases. Data from publications was also used when a complete set of conditions was available in the paper. Overall, the model gives a reasonable prediction under a multitude of conditions. Some of the comparisons are presented in this section.

FIGURE 2 shows the model predictions vs. experiment results for pure CO<sub>2</sub> corrosion in a single phase flow loop system. Fairly good agreement can be seen between model predictions and experimental results under various pH and flow velocities, indicating that the corrosion process, especially transport phenomenon is properly simulated by the model. It is apparent that at lower pH (pH= 4), the corrosion rate is more sensitive to the change of flow velocity. This is because that at lower pH, the major corrosive specie is H<sup>+</sup>, the reduction reaction of which is controlled by mass transfer, while at higher pH, H<sub>2</sub>CO<sub>3</sub> reduction becomes dominant, a process that is mainly limited by chemical reaction, and therefore not so sensitive to velocity change.

FIGURE 3 illustrates the comparison between the model and experiments for different partial pressure of CO<sub>2</sub>. Clearly, good agreement is achieved under various test conditions. It is shown that increased CO<sub>2</sub> partial pressure promotes the corrosion rate under test conditions. This can be explained by the fact that increased CO<sub>2</sub> partial pressure leads to higher concentration of H<sub>2</sub>CO<sub>3</sub> in the solution, and therefore increases the H<sub>2</sub>CO<sub>3</sub> reduction rate. However, this trend does not always hold, e.g. higher CO<sub>2</sub> partial pressure does not necessarily lead to higher corrosion rate. In film forming conditions, increased CO<sub>2</sub> partial pressure facilitates the formation of iron carbonate film and therefore reduces the corrosion rate.

FIGURE 4 gives the comparison between the model and the experiments for CO<sub>2</sub>/HAc mixed corrosion. Experimental results show that as HAc concentration increases, the corrosion rate is enhanced. This trend is correctly captured by the model. Reasonable match can be seen for different levels of HAc concentration.

FIGURE 5 shows comparison between predicted and measured<sup>6</sup> corrosion rates for mixed CO<sub>2</sub>/H<sub>2</sub>S corrosion. The test conditions are tabulated in TABLE 1. It can be seen that these cases reflect a wide range of conditions in terms of critical factors affecting corrosion, such as temperature, partial pressures of CO<sub>2</sub> and H<sub>2</sub>S. Good agreement between the model and the experimental results is still observed reflecting the sound theoretical base of the model.

FIGURE 6 shows the potentiodynamic sweep given by the model and that obtained in the experiment. SHE in the y-axis title of the figure stands for the standard hydrogen electrode. A good match of the potentiodynamic sweep curve reveals that the electrochemical nature of corrosion process is properly simulated by the model, and therefore the reliable prediction can be expected. In addition, the model provides sweep curves for individual anodic and cathodic reactions involved in the corrosion process as well as those for total anodic and cathodic reactions, the information which can not be obtained by experimental means. This information offers a powerful tool in analyzing the corrosion mechanism.

FIGURE 7 displays a concentration profile of H<sub>2</sub>S as a function of distance from steel surface for a case of H<sub>2</sub>S corrosion. It can be seen that different concentration gradients exist within three layers on steel surface. Clearly, inner mackinawite film offers the highest mass transfer resistance in this scenario. This is usually the case at the very beginning of corrosion process when H<sub>2</sub>S reacts with iron surface to form a very thin but dense and protective mackinawite film, and corrosive species can only travel through it

by solid state diffusion. It can be shown that as corrosion proceeds, a thicker and porous outer mackinawite layer will be generated on top of the inner mackinawite film. The tortuous passage within this layer largely slows down the transport of corrosive species and will dominate the corrosion process, as demonstrated in FIGURE 8.

## MODEL LIMITATIONS

The inputs of the model include: temperature, pressure, pipe diameter, liquid velocity, pH and concentrations of corrosive species such as CO<sub>2</sub>, H<sub>2</sub>S, HAc and O<sub>2</sub>. The concentration of Fe<sup>2+</sup> is also required for the calculation of FeCO<sub>3</sub> film growth kinetics. In case H<sub>2</sub>S exists in the system, the total time of corrosion process is needed since time evolution is involved in H<sub>2</sub>S model. Based on specific input values, the model calculates the uniform corrosion rate and determines the contribution of corrosive species to overall corrosion rate. The recommended range of inputs is given by the model based on the range of parameters tested. Inputs beyond this range are allowed but accuracy of the prediction is not guaranteed. The recommended range of inputs defined in the model is listed below,

Temperature: 1 to 120°C

Pipe diameter: 0.01 to 1 m

Liquid velocity: 0.001 to 20 m/s

Fe<sup>2+</sup>: 0 to 100ppm

HAc: 0 to 1000ppm

pH: 3 to 7

O<sub>2</sub>: 0 to 10000ppm

H<sub>2</sub>S and CO<sub>2</sub>: sum of partial pressure of H<sub>2</sub>S and CO<sub>2</sub> is no greater than total system pressure.

In this initial version of model, a number of factors have not yet been taken into consideration. These factors limit the use of this model under certain circumstances. Major limitations associated with current version of the model are listed below,

- This model is a so-called “point model”, corrosion rates are predicted based on conditions for a single point on the metal surface, e.g. somewhere along the pipeline where the operating conditions are known. The accuracy of the prediction heavily depends on the reliability of the parameters provided to the model.
- This model is developed currently to only take into account the effect of single-phase flow; multiphase flow module is not available at present; however object-oriented programming of this model may enable existing corrosion modules to be coupled with external flow simulators such as OLGA<sup>(4)</sup>, FLUENT<sup>(5)</sup>, etc.
- This model predicts uniform corrosion; no localized corrosion module has been included at present.
- This model assumes simple water chemistry, i.e. the infinite solution theory is invoked and an ideal solution is assumed; furthermore the interaction between the chemical and diffusional processes is ignored meaning that the species independently diffuse through the boundary layer without interacting with each other.

---

<sup>(4)</sup> OLGA is a trademarked product of SPT Group.

<sup>(5)</sup> FLUENT is a trademarked product of Fluent Inc.

- This model employs a simple empirical correlation based on supersaturation of iron carbonate to simulate iron carbonate film growth which is subject to further development.
- This model does not take into account the effect of high solution salinity on corrosion process.
- A simple criterion is used to determine the transition between CO<sub>2</sub> dominated and H<sub>2</sub>S dominated corrosion. When CO<sub>2</sub> and H<sub>2</sub>S coexist, corrosion rates are calculated based on both CO<sub>2</sub> and H<sub>2</sub>S corrosion mechanism as described earlier, the corrosion rates are then compared with each other. The mechanism that gives the higher corrosion rate is considered as the dominated mechanism.
- No data post processing is available in this model.

Most of the limitations listed above will be overcome in the near future as work on the model continues and as the involvement from the broader corrosion community initiates.

## **CONCLUSIONS**

An open-source mechanistic model has been developed in this work to predict the uniform corrosion rate of carbon steel in the environment containing carbon dioxide, hydrogen sulfide, organic acid and/or oxygen.

Corrosion process can be altered by adding/removing any particular reactions to/from the system, including user-defined reactions to accommodate different corrosion environments.

The model has been calibrated with a large experimental database and was found to give satisfactory predictions under various conditions.

## **REFERENCES**

1. R. Nyborg, "Overview of CO<sub>2</sub> Corrosion Models for Wells and Pipelines", Corrosion/2003, Paper No. 02233. (Houston, TX: NACE 2003)
2. S. Netic, J. Postlethwaite and S. Olsen, Corrosion Science, "An Electrochemical Model for Prediction of Corrosion of Mild Steel in Aqueous Carbon Dioxide Solutions", Vol. 52, No.4, 1996, p.280-294.
3. K. George and S. Netic, "Electrochemical Investigation and Modeling of Carbon Dioxide Corrosion of Carbon Steel in the Presence of Acetic Acid", Corrosion/2004, Paper No. 04379. (Houston, TX: NACE 2004)
4. W. Sun and S. Netic, "A Mechanistic Model of H<sub>2</sub>S Corrosion of Mild Steel", Corrosion/2007, Paper No. 07655. (Houston, TX: NACE 2007)
5. C. de Waard and D. E. Milliams, Corrosion, 31 (1975): p.131.
6. I. H. Omar, Y. M. Gunaltun, J. Kvarekval and A. Dugstad, "Corrosion of Carbon Steel Under Simulated Kashagan Field Conditions", paper No. 05300. (Houston, TX: NACE 2005)

**TABLE 1**  
**THREE CASES OF TEST CONDITIONS**

Parameters	Case 1	Case 2	Case 3
Temperature, °C	80	25	80
pCO <sub>2</sub> , bar	3.3	3.3	10.0
pH <sub>2</sub> S, bar	10	10	30
Solution pH	3.10	3.20	2.90
Pipe diameter, m	0.015	0.015	0.015
Velocity, m/s	1	1	1
Duration, days	19	21	15

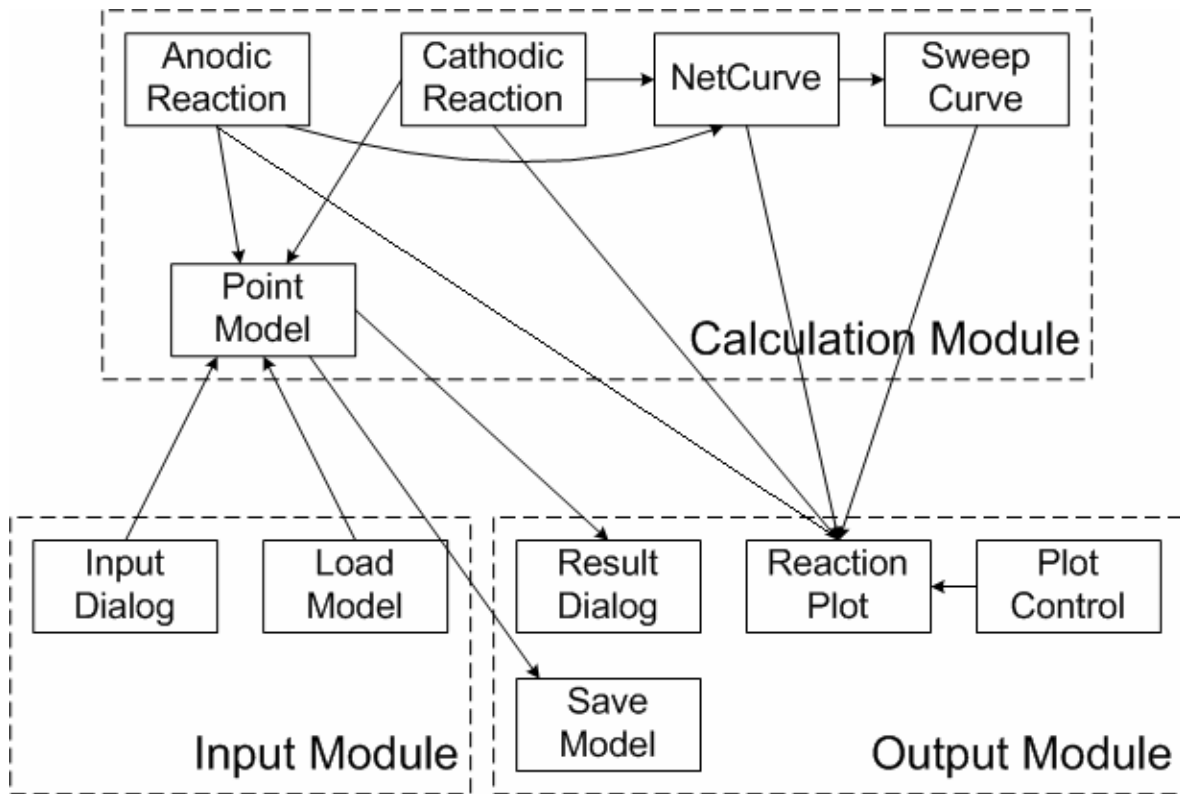


FIGURE 1 Architecture of the Model

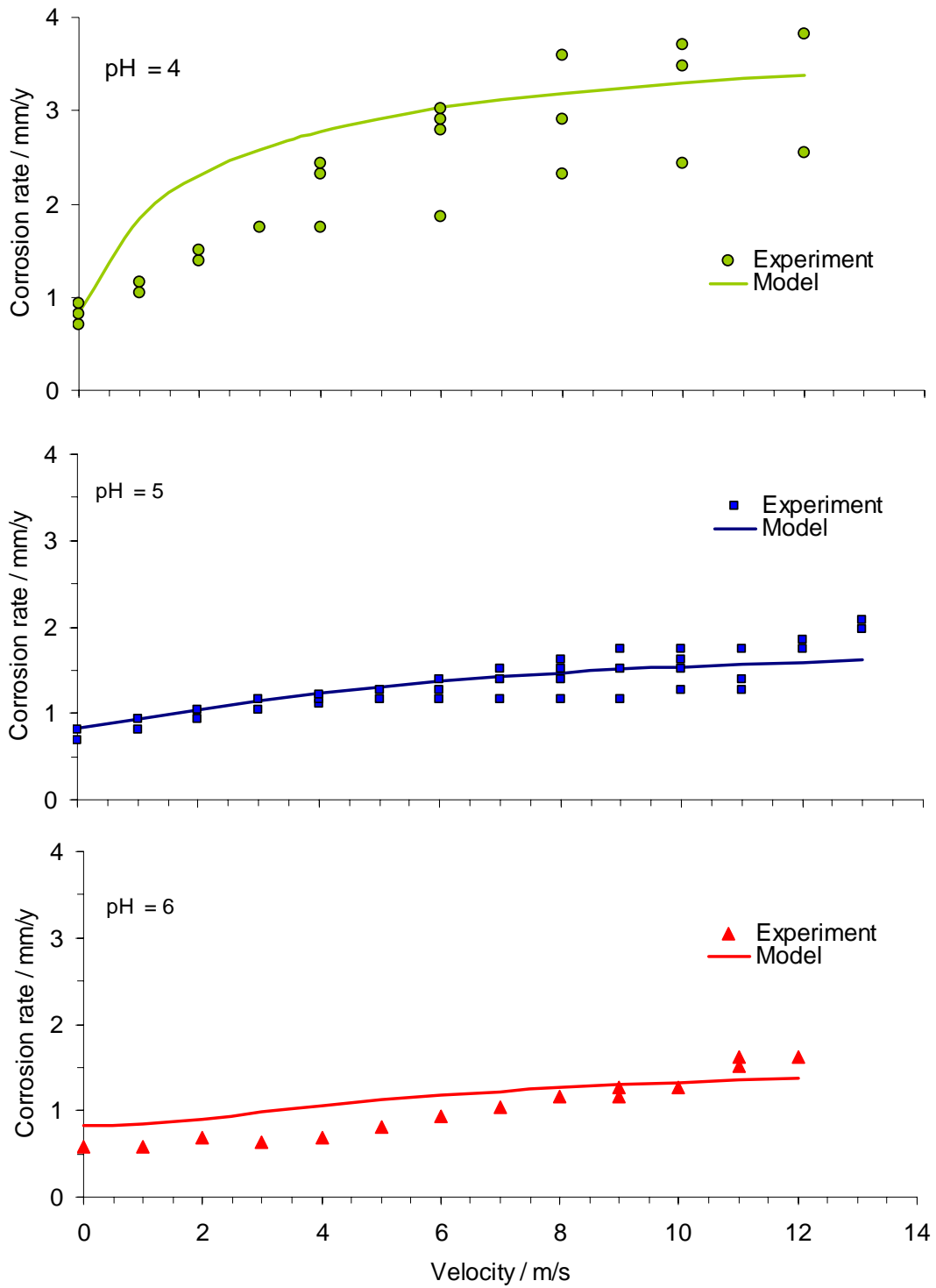


FIGURE 2 Comparison of predicted and experimentally measured corrosion rates at different velocities. Test conditions: 20°C, partial pressure of CO<sub>2</sub> 1 bar, pipe diameter 0.015 m.

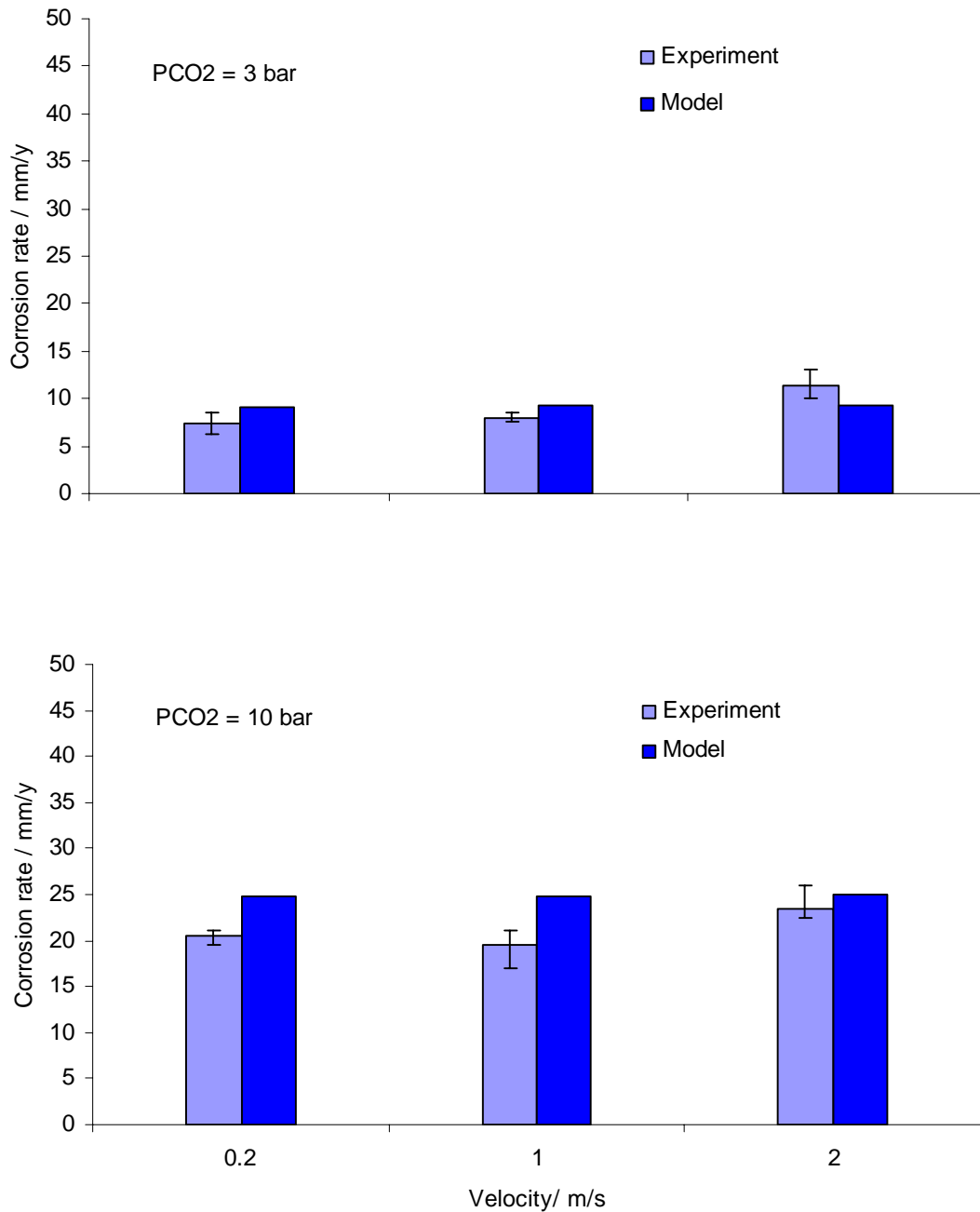


FIGURE 3 Comparison between the model and experiments for different partial pressure of  $CO_2$ . Test condition: temperature  $60^\circ C$ , pH 5, pipe diameter 0.1 m.

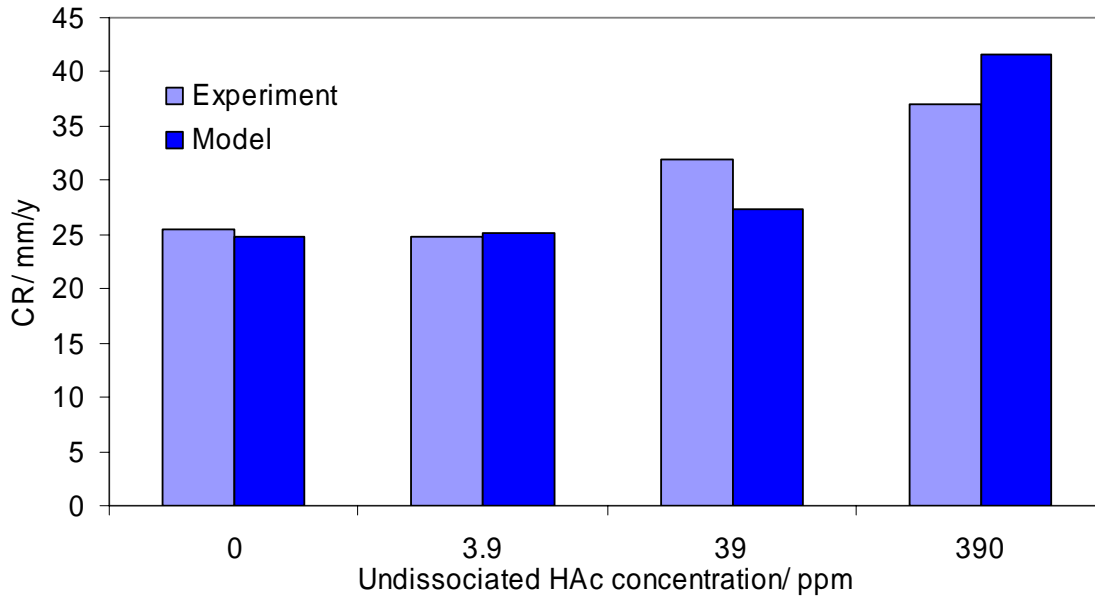


FIGURE 4 Comparison of experimental and predicted corrosion rate. Test conditions: temperature 60°C, pH 5, liquid velocity 1 m/s, partial pressure of CO<sub>2</sub> 10 bar, pipe diameter 0.1m. Data is taken from ICMT database.

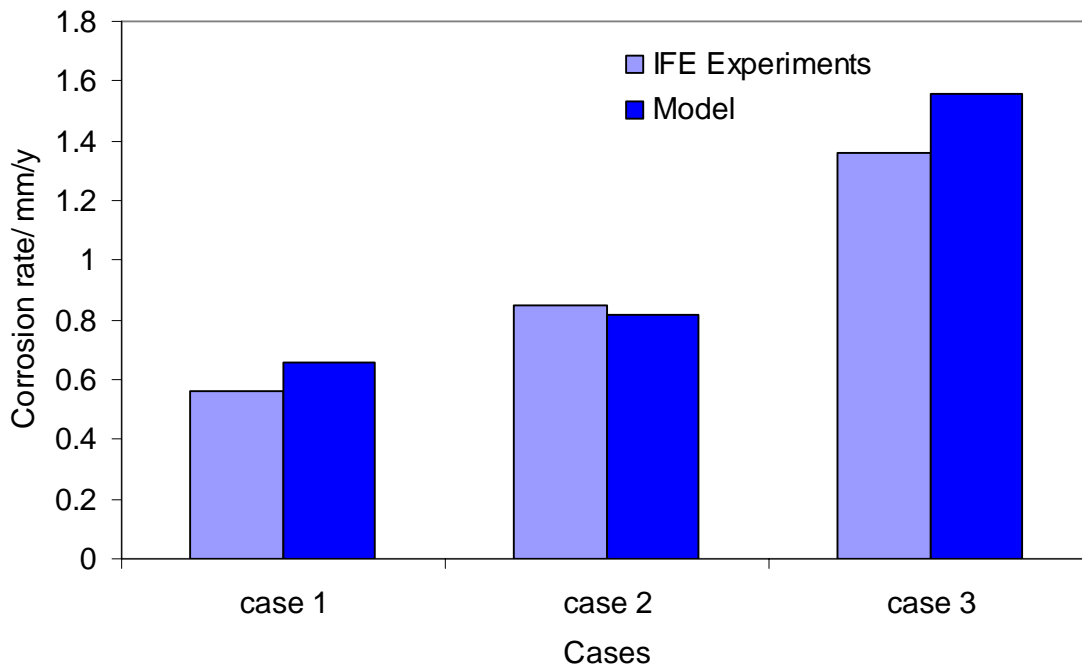


FIGURE 5 Comparison of experimental and predicted corrosion rate under the conditions listed in TABLE 1.

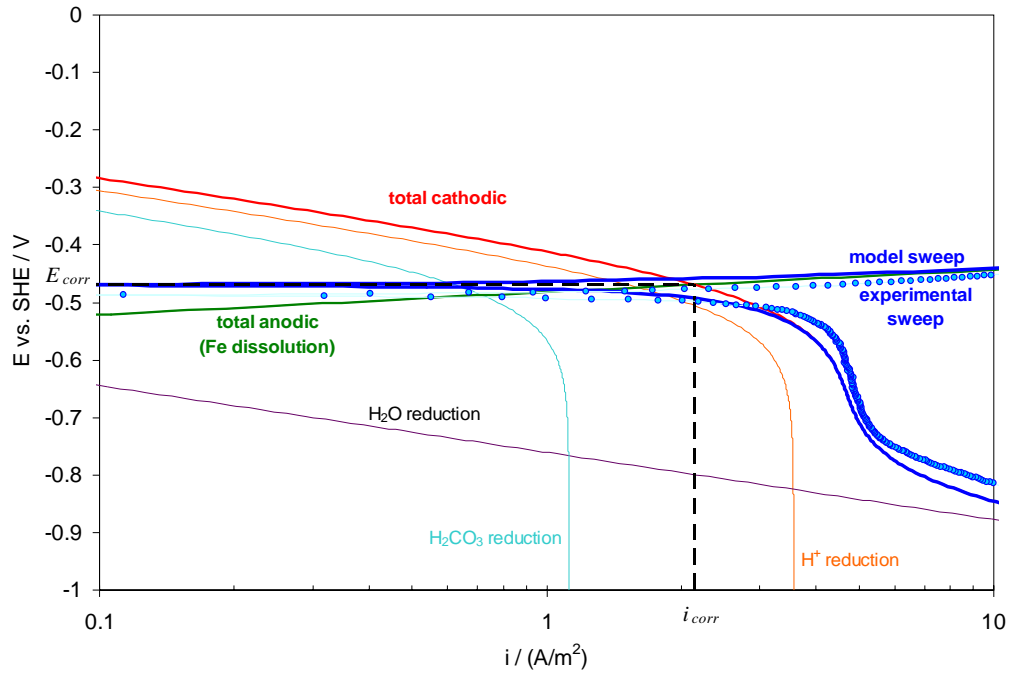


FIGURE 6 Comparison of experimental and predicted potentiodynamic for a case of temperature 20°C , partial pressure of CO<sub>2</sub> 1bar, solution pH 4 and velocity 2 m/s.

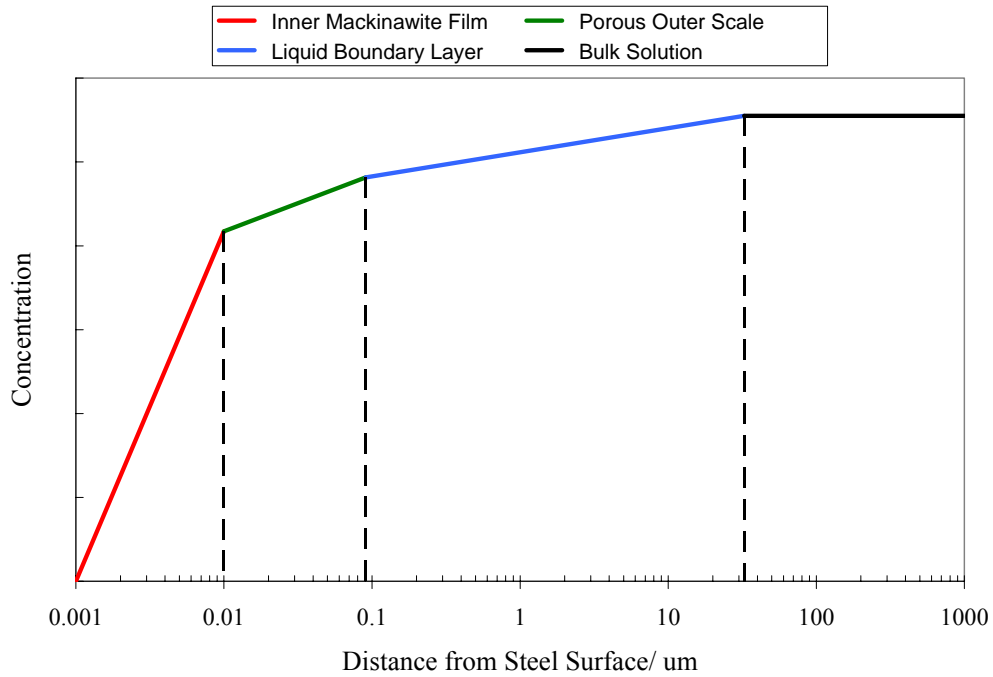


FIGURE 7 Predicted H<sub>2</sub>S concentration (mmol/L) profile at 4 seconds. Test conditions: temperature 20°C, partial pressure of CO<sub>2</sub> 1bar, pipe diameter 0.1m, liquid velocity 1m/s, solution pH 4 and partial pressure of H<sub>2</sub>S 0.5 bar.

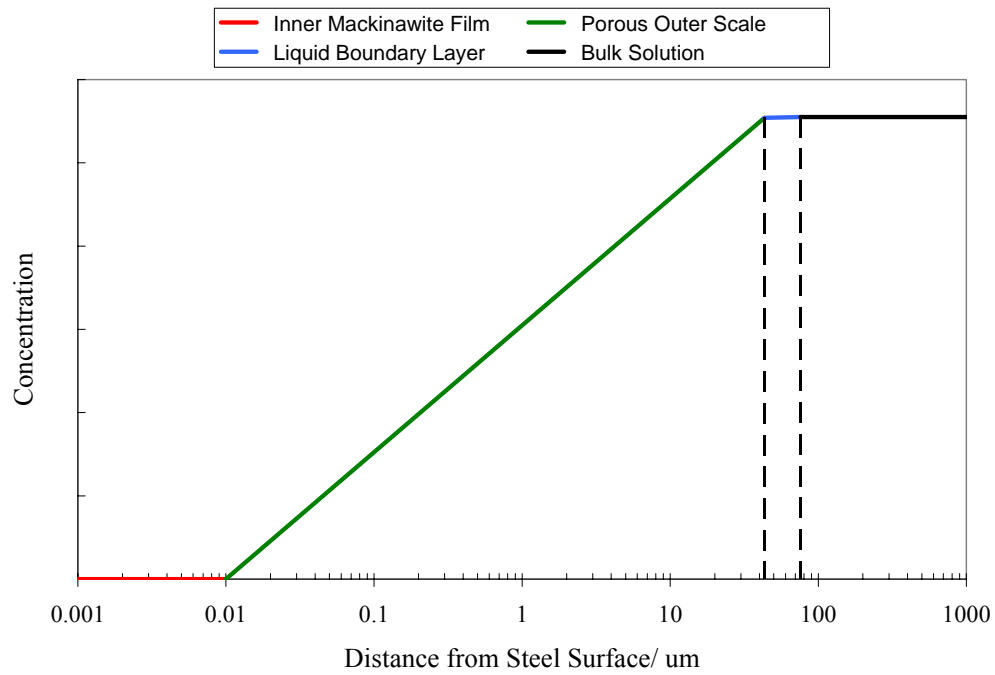


FIGURE 8 Predicted H<sub>2</sub>S concentration (mmol/L) profile at 24 hours. Test conditions: temperature 20°C, partial pressure of CO<sub>2</sub> 1bar, pipe diameter 0.1m, liquid velocity 1m/s, solution pH 4 and partial pressure of H<sub>2</sub>S 0.5 bar.